# Head-to-head comparison of the hybrid tracer indocyanine green-Tc-99m-nanocolloid with(99m)Tc-Senti-Scint using sentinel node lymphoscintigraphy and single-photon emission computed tomography combined with computer tomography in melanoma

Rietbergen, D.D.D.; Meershoek, P.; Kleinjan, G.H.; Donswijk, M.; Olmos, R.A.V.; Leeuwen, F.W.B. van; ... ; Hage, J.A. van der

Original article

Nuclear Medicine Communications

# Head-to-head comparison of the hybrid tracer indocyanine green-$^{99m}$Tc-nanocolloid with $^{99m}$Tc-Senti-Scint using sentinel node lymphoscintigraphy and single-photon emission computed tomography combined with computer tomography in melanoma

Daphne D.D. Rietbergen[a,b], Philippa Meershoek[a,c], Gijs H. KleinJan[a,c], Maarten Donswijk[d], Renato A. Valdés Olmos[a,b], Fijs W.B. van Leeuwen[a,c], Martin W.M.C. Klop[c] and Jos A. van der Hage[e,f]



***Objective*** **The hybrid tracer indocyanine green (ICG)-$^{99m}$Tc-nanocolloid has been introduced for sentinel node imaging. However, until now, a comparison of this tracer with other radiocolloids with a larger particle size has not been effectuated. Based on a head-to-head evaluation in patients with melanoma, we have compared ICG-$^{99m}$Tc-nanocolloid (particle size 5–80 nm) with $^{99m}$Tc-Senti-Scint (particle size 100–600 nm) to establish differences in drainage pattern and sentinel node localization using lymphoscintigraphy and single-photon emission computed tomography combined with computer tomography (SPECT-CT) in melanoma patients scheduled for sentinel node biopsy.**

***Methods*** **Twenty-five patients (mean age: 56.9 years, range: 25–79 years) with a melanoma scheduled for SLN biopsy prior to (re)excision of the primary lesion (scar) were prospectively included following a two-day procedure. The first day, after $^{99m}$Tc-Senti-Scint injection in four intradermal depots around the primary lesion or scar, early/delayed lymphoscintigraphy and SPECT-CT images were acquired. The injection sites were marked. The second day, after assessing lymph node radioactivity using planar scintigraphy, ICG-$^{99m}$Tc-nanocolloid was injected at the previously marked skin points and imaging was performed. The paired planar and SPECT-CT images of both tracers were evaluated with respect to drainage patterns, SLN visualization and non-SLN appearing.**

***Results*** **Twenty-four out of 25 patients were evaluable. SLN visualization on a patient basis was 100% for ICG-$^{99m}$Tc-nanocolloid and 96% for $^{99m}$Tc-Senti-Scint, whereas uptake in non-SLNs was found in, respectively, 71% (17/24) and 61% (14/23). Concordance in drainage to 45 lymph node basins was 91%. Discordant drainage was found for two melanomas in the head-and-neck and one in the clavicular area. Unique lymph node basins were seen in 44/45 (98%) for ICG-$^{99m}$Tc-nanocolloid and 42/45 (93%) for $^{99m}$Tc-Senti-Scint. Concerning identified SLNs, the number was similar for both tracers ($n$=58); however, more non-SLNs (65 vs 50) were visualized with ICG-$^{99m}$Tc-nanocolloid than with $^{99m}$Tc-Senti-Scint.**

***Conclusion*** **A slightly higher SLN visualization accompanied by a tendency to depict more non-SLNs was found for ICG-$^{99m}$Tc-nanocolloid. Excepting the head and neck area, an overall high concordance in drainage was found for both radiotracers. With an additional value for the hybrid tracer due to the combination of preoperative imaging and the additional visual signal in the operation room, added by the fluorescent component of the hybrid tracer, there was a preference for ICG-$^{99m}$Tc-nanocolloid.**


**Nuclear Medicine Communications** 2020, **41**:1010–1017

**Keywords: image-guided surgery, melanoma, radiocolloids, sentinel node,**

[a]Interventional Molecular Imaging Laboratory, [b]Nuclear Medicine Section, Department of Radiology, Leiden University Medical Center, Leiden, Departments of [c]Head and Neck Surgery and Oncology, [d]Nuclear Medicine, [e]Surgical Oncology, Netherlands Cancer Institute, Amsterdam and [f]Department of Surgery, Leiden University Medical Center, Leiden, The Netherlands

Correspondence to Daphne D.D. Rietbergen, MD, Nuclear Medicine Section, Department of Radiology, Leiden University Medical Center, Leiden, Albinusdreef 2, 2300 RC Leiden, The Netherlands
Tel: +31 71 5261874; fax: +31 71 5264649;
e-mail: d.d.d.rietbergen@lumc.nl

**Received** 26 May 2020 **Accepted** 23 June 2020

## Introduction

A unique aspect of lymphatic mapping procedures is that they are able to minimally invasively target the lymphatic drainage pathways of primary tumors. This procedure helps to accurately identify sentinel lymph nodes (SLNs) that can harbor micrometastases in node-negative patients following biopsy [1]. While there are discussions ongoing with regard to the clinical value of subsequent lymph node dissections in these patients, there is consensus that identification of early lymphatic micrometastases holds the prognostic value by increasing the rate of regional disease control. Furthermore, positive


DOI: 10.1097/MNM.0000000000001256

node(s) indicates which patients are eligible for adjuvant treatment with immunotherapy. Extensive lymph node dissection increases the rate of regional disease control and provides prognostic information but does not increase melanoma-specific survival among patients with melanoma and sentinel-node metastases [2]. Following the introduction of the approach by Cabañas [3], the modernization of the sentinel concept by Morton *et al.* [4] led to personalized nodal identification and biopsy with a minimal chance of side effects in breast cancer and melanoma care [5,6]. The same approach, complemented by single-photon emission computed tomography combined with computer tomography (SPECT-CT), has been incorporated for the sentinel node procedure in head-and-neck surgery [7,8], gynecology [9] and urology [10,11].

Despite the success of the hybrid tracer indocyanine green (ICG)-$^{99m}$Tc-nanocolloid in targeting of the SLNs [12,13], overflow to higher echelon nodes (non-SLNs) is still observed. One reason for this is could be a discrepancy between drainage speed and the volume/quantity of contrast administered. Such discrepancy occurs, especially in areas of complex anatomy like the head-and-neck, parts of the trunk and pelvis [14,15]. Preoperative imaging based on a combination of sequential scintigraphy and SPECT-CT allows for an accurate discrimination of the true SLNs from non-SLNs [16,17]. With the addition of ICG to $^{99m}$Tc-nanocolloid, the intraoperative search of SLNs in complex anatomic areas has been simplified thanks to the use of a fluorescence camera in combination with gamma-devices [12]. This hybrid approach with preoperative SLN mapping using lymphoscintigraphy and SPECT-CT as a roadmap to identify SLNs in the operation room may obviate the application of surrogate markers such as the 10% rule [18–20] by surgeons. In the future, the development of tracers that only accumulate in SLNs would significantly simplify the procedures by transforming the prevailing imaging paradigm 'not all radioactive nodes are sentinel nodes' to an alternative one resting on 'all radioactive lymph nodes are sentinel nodes' [21].

It is well known that radiocolloids like ICG-$^{99m}$Tc-nanocolloid with a particle size varying from 5 to 80 nm have an enhanced SLN specificity compared to small molecule dyes (e.g., patent blue diameter +1 nm) and dyes such as ICG that interact with native human serum albumin (+7 nm) [22,23]. On the other hand, because lymphatic distribution and nodal filtration are influenced by particle size, there is a tendency to reduce the number of non-SLNs by using radiocolloids with a larger size [24]. This rationale has provided the basis for the development of radiocolloids with a larger particle size such as $^{99m}$Tc-Senti-Scint (diameter 100–600 nm). However, until now, it has not been documented if in fact radiocolloids with a larger particle size yield superior performance.

Given all the above-mentioned variables that can influence lymphatic flow of a radiocolloid, in analogy to the setup previously used to validate the similarity of lymphatic drainage for $^{99m}$Tc-nanocolloid and ICG-$^{99m}$Tc-nanocolloid [25], we have now compared the differences in drainage patterns of $^{99m}$Tc-Senti-Scint and ICG-$^{99m}$Tc-nanocolloid. We decided to perform this comparison on the basis of a head-to-head evaluation using lymphoscintigraphy and SPECT-CT in melanoma patients scheduled for SLN biopsy. Furthermore, we studied whether the increased particle size could reduce the amount of non-SLNs, while preserving the SLN identification

## Material and methods

### Patient demographics

The trial was initially registered as the prospective study N13ICG ($^{99m}$Tc-Senti-Scint vs ICG-$^{99m}$Tc-nanocolloid for sentinel node biopsy of malignant melanoma of the trunk, of an extremity or in the head and neck) at the Netherlands Cancer Institute – Antoni van Leeuwenhoek Hospital. Following the approval of the protocol review board of the institution, the study was activated on 16 June 2014 as the trial NL4568 in the Netherlands Trial Register, and closed on 30 November 2017.

Twenty-five patients (mean age: 56.9 years, range: 25–79 years) with a melanoma scheduled for SLN biopsy prior to (re)excision of the primary lesion (scar) were prospectively included after informed consent. One patient with a nose melanoma was excluded since the SPECT-CT data were not completed, meaning twenty-four patients were evaluated. The localization of the primary lesion was as follows: head-and-neck region ($n = 5$), the trunk ($n = 11$) and extremities ($n = 8$).

## Methods

### Imaging procedure

All patients followed a two-day procedure. On the first day, 90 MBq (±10%; 2.43 mCi) $^{99m}$Tc-Senti-Scint was injected in four intradermal depots around the primary lesion or scar. Injection points were marked on skin with indelible ink to facilitate reproducibility in the administration of the second tracer. Lymphatic drainage was mapped using dynamic lymphoscintigraphy (0–10 min), static lymphoscintigraphy (15 min and 2 h postinjection) and SPECT-CT (2 h postinjection). The second day, after planar images to control resting lymph node radioactivity, 90 MBq (±10%; 2.43 mCi) ICG-$^{99m}$Tc-nanocolloid was injected and similar images were acquired. The paired planar and SPECT-CT images of both tracers were evaluated with respect to drainage to lymph node basins, SLN visualization and non-SLN uptake. Both lymphoscintigraphy and SPECT-CT were acquired using a hybrid system (Symbia T6, Siemens, Erlangen, Germany). The flowchart of the study setup is presented in more detail in Fig. 1.

**Fig. 1**

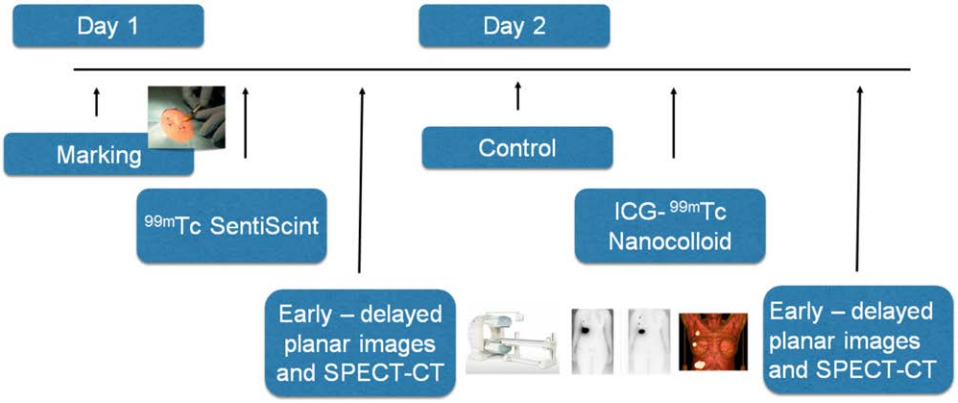


Flowchart of the study design. The first day, four intradermal depots $^{99m}$Tc-Senti-Scint ware injected around the primary lesion or scar after marking the skin points. Early and delayed planar lymphoscintigraphy and SPECT-CT were acquired. The second day, after planar images to control resting lymph node radioactivity, ICG-$^{99m}$Tc-nanocolloid was injected at the previously marked skin points. The same image acquisitions were acquired for both tracers and reviewed by two experienced nuclear medicine physicians.



### Comparison imaging findings indocyanine green-$^{99m}$TC-nanocolloid and $^{99m}$Tc-Senti-Scint and scoring

The derived early, delayed planar and SPECT-CT data of both the tracers were reviewed by two experienced nuclear medicine physicians. The number of drainage basins, numbers of SLNs, non-SLNs and their anatomical localization were scored. The first lymph node on which a tumor drains is considered to be the sentinel node. The early, delayed planar and SPECT-CT images of both tracers were compared to each other and scored on concordant or discordant findings.

### Surgical guidance

Planar images were used to mark the location of identified SLNs on the skin, while SPECT-CT images were used to indicate the anatomical SLN location in relation to muscles and vessels in the draining lymph node basin. Figure 1 shows the flowchart of the study. For the intraoperative procedure, only the findings of the ICG-$^{99m}$Tc-nanocolloid study were used. Following gamma-probe (Neoprobe, Johnson&Johnson Medical, Hamburg, Germany) localization at the indicated SLN site, SLNs were further prepared and removed under guidance of a fluorescent camera (PhotoDynamic Eye, Hamamatsu Photonics, Hamamatsu, Japan) as previously described [12].

## Results

The SLN visualization rate on a patient basis was 100% for ICG-$^{99m}$Tc-nanocolloid and 96% for $^{99m}$Tc-Senti-Scint due to nonvisualization in one patient in the latter group. Drainage to 45 unique lymph node basins was seen with a concordant rate of 91% between both the tracers. Uptake in non-SLNs was found in, respectively, 71% (17/24) and 61% (14/23) of patients (Table 1 and Fig. 2). The concordance of drainage basins was 100% for melanomas located in extremities.

Discordant findings were mainly seen in the head-and-neck area, whereas two out of five patients showed discrepancy between the images of both tracers (Fig. 3). In one patient with a midline nose melanoma, the images showed bilateral neck drainage with tracer concordance for the right side but discordant findings on the left side with an extra submandibular sentinel lymph node visualized only with $^{99m}$Tc-Senti-Scint (Fig. 4). In the other case, a patient with a melanoma of the skin (parietotemporal region), the images of both tracers showed a lymph node in region 2 of the neck, with an additional lymph node (in the parotic area) between the injection site and the previously mentioned concordant SLN only seen on the ICG-$^{99m}$Tc-nanocolloid (Fig. 5).

Moreover, the only patient with a nonconcordant study in the trunk was a patient with a melanoma in the clavicular area (Fig. 6), which is an area adjacent to the neck also characterized by a high degree of unpredictable drainage. In the three patients where discordance was seen between the two radiotracers, the pathologic examination did not reveal any micro- or macrometastasis.

## Discussion

In this study, two different radiocolloids for SLN imaging were compared to document lymphatic drainage in relation to particle size in a head-to-head designed approach in patients with melanoma scheduled for SLN biopsy. Related to lymph node basin, an overall 91% drainage concordance was found. The concordance of drainage basins was 100% for melanomas located in extremities.

The sentinel node visualization rate was 100% for ICG-$^{99m}$Tc-nanocolloid and 96% for $^{99m}$Tc-Senti-Scint with

**Table 1** Schematic overview of the results of the 24 which could be evaluatedPatient (gender, age)

| | | Basin(s) (number) | | SN(s) (number) | | Non-SN | |
|---|---|---|---|---|---|---|---|
| | Primary lesion site | $^{99m}$Tc-Senti-Scint | ICG-$^{99m}$Tc-nanocolloid | $^{99m}$Tc-Senti-Scint | ICG-$^{99m}$Tc-nanocolloid | $^{99m}$Tc-Senti-Scint | ICG-$^{99m}$Tc-nanocolloid |
| Head and neck | | | | | | | |
| 1 (M, 68 years) | Cheek | 2 | 2 | 2 | 2 | – | – |
| 2 (F, 42 years) | Parietotemporal | 1 | 2 | 1 | 2 | – | – |
| 3 (F, 57 years) | Occipital | 3 | 3 | 3 | 3 | + | + |
| 4 (M, 72 years) | Nose | 3 | 3 | 3 | 3 | + | + |
| 5 (M, 55 years) | Nose | 3 | 2 | 5 | 4 | – | – |
| Extrimities | | | | | | | |
| 1 (F, 79 years) | Hand | 2 | 2 | 4 | 4 | + | + |
| 2 (F, 35 years) | Upper leg | 1 | 1 | 1 | 1 | + | + |
| 3 (F, 51 years) | Upper arm | 1 | 1 | 1 | 1 | + | + |
| 4 (F, 51 years) | Upper leg | 1 | 1 | 1 | 1 | + | + |
| 5 (M, 64 years) | Lower leg | 1 | 1 | 1 | 1 | + | + |
| 6 (M, 58 years) | Upper leg | 1 | 1 | 2 | 2 | + | + |
| 7 (M, 68 years) | Upper leg | 1 | 1 | 2 | 2 | + | + |
| 8 (M, 54 years) | Upper leg | 1 | 1 | 2 | 2 | + | + |
| Trunk | | | | | | | |
| 1 (F, 58 years) | Shoulder | 1 | 1 | 2 | 2 | – | – |
| 2 (F, 36 years) | Back | 1 | 1 | 1 | 1 | – | + |
| 3(M, 74 years) | Back | 2 | 2 | 2 | 2 | – | + |
| 4 (M, 67 years) | Upper back | 4 | 4 | 4 | 4 | – | – |
| 5 (M, 50 years) | Back | 2 | 2 | 3 | 3 | + | + |
| 6 (M, 66 years) | Upper back | 4 | 4 | 4 | 4 | – | – |
| 7 (M, 68 years) | Upper back | 1 | 1 | 1 | 1 | + | + |
| 8 (M, 55 years) | Upper back | 3 | 3 | 6 | 6 | + | + |
| 9 (F, 56 years) | Trunk | 2 | 2 | 2 | 2 | – | – |
| 10 (M, 25 years) | Gluteal | 1 | 1 | 1 | 1 | + | + |
| 11 (M, 47 years) | Clavicular area | 0 | 2 | 0 | 2 | – | + |
| *N*=24 patients | | *N*=42 basins | *N*=44 basins | *N*=54 SN | 24/24=100% | 14/23=61% | 17/24=71% |
| Mean age=56 years | | 42/45=93% | 44/45=98% | 23/24=96% | *N*=56 sentinel node | | |
| Range=25–79 years | | -HN=12 | -HN=12 | -HN=14 | -HN=14 | | |
| | | -Ext=9 | -Ext=9 | -Ext=14 | -Ext=14 | | |
| | | -Trunk=21 | -Trunk=23 | -Trunk=26 | -Trunk=28 | | |

Ext, extrimities; F, female; HN, head and neck; ICG, indocyanine green; M, male; +, Non-SN present; -, Non-SN absent.

**Fig. 2**

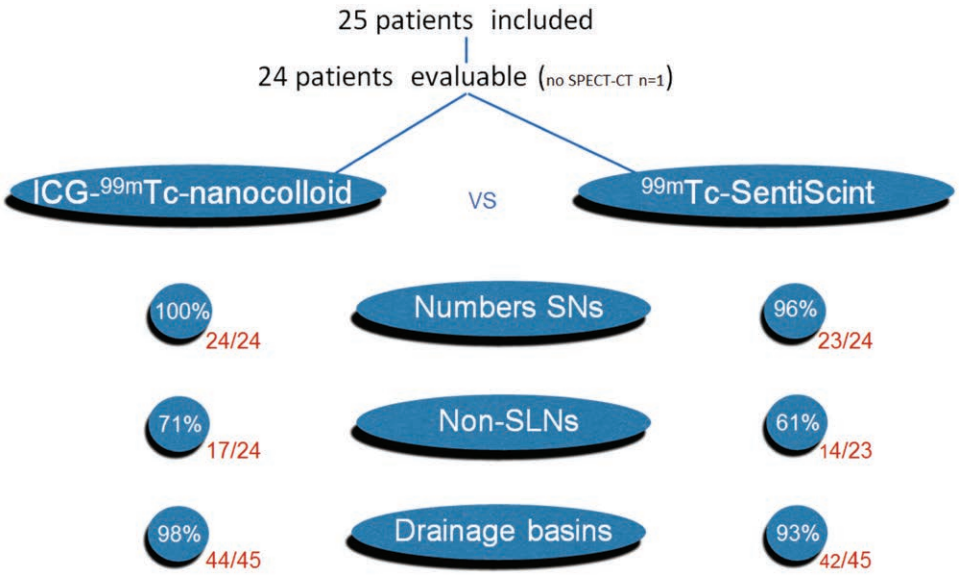


Schematic overview of the results. Of the 25 patients which were included, 24 patients could be evaluated. SLN visualization rate on a patient basis was 100% for ICG-$^{99m}$Tc-nanocolloid and 96% for $^{99m}$Tc-Senti-Scint due to one nonvisualization. Concerning the overall number of SLNs identified, this was 56 with ICG-$^{99m}$Tc-nanocolloid and 54 (96%) with $^{99m}$Tc-Senti-Scint. Uptake in non-SLNs was found in, respectively, 71 and 61% of the patients. Drainage to 45 unique lymph node basins was seen with a concordant rate of 91%. ICG, indocyanine green; SLN, sentinel lymph node.

**Fig. 3**

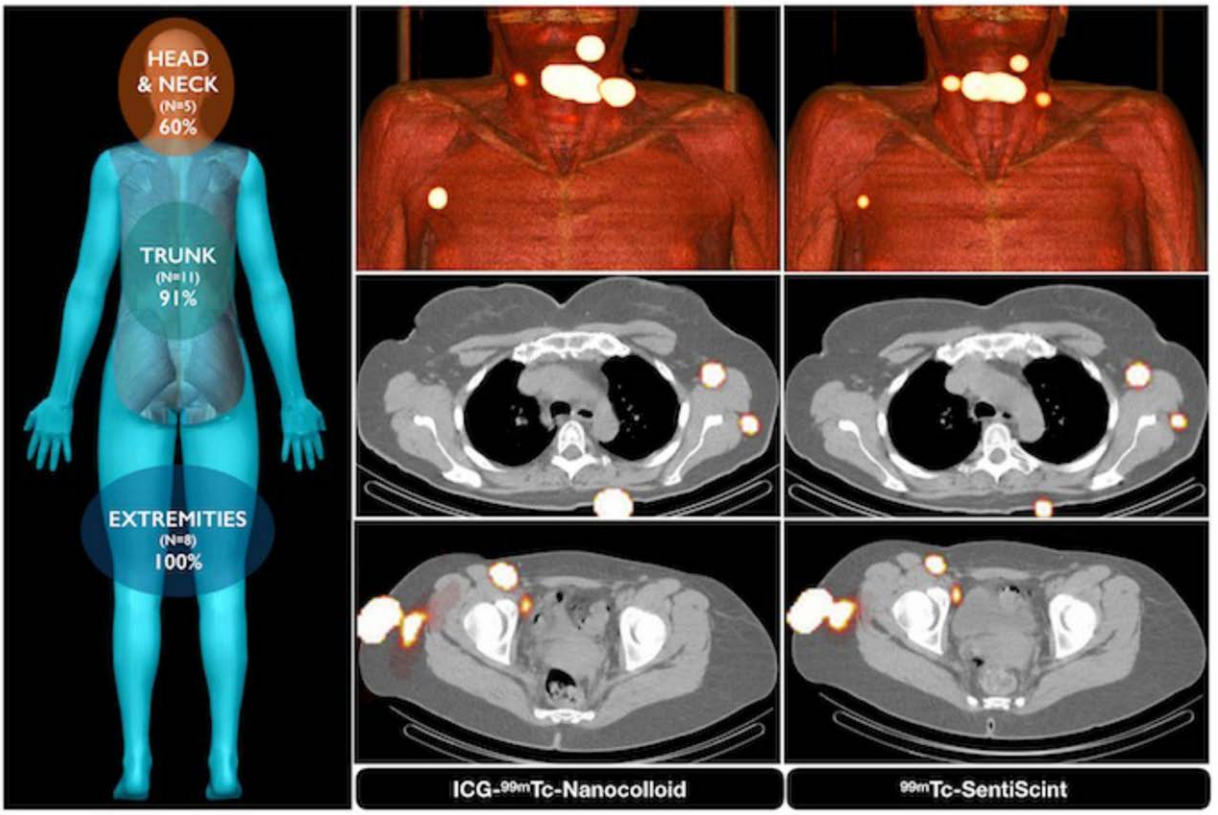


On the left, lymphatic drainage concordance rate between ICG-$^{99m}$Tc-Nanocolloid and $^{99m}$Tc-Senti-Scint related to the primary melanoma location varying from 100% for extremities to 60% for head/neck. Discordant findings were seen in two out of five patients with melanomas in the head and neck area. In one patient, there was a nonvisualization in a Senti-Scint patient in trunk melanoma (clavicular region). On the right, SPECT-CT-based examples of concordance for melanomas of the midline of the neck showing drainage to three cervical lymph node stations and the right axilla (upper row), left medial upper back with drainage to sentinel nodes in the left scapular area and left axilla (middle row) and lateral right upper leg with drainage to an inguinal sentinel node and an iliac second-tier node on the right (lower row). ICG, indocyanine green; SPECT-CT, single-photon emission computed tomography combined with computer tomography.

slightly higher non-SLNs for ICG-$^{99m}$Tc-nanocolloid group. Based on these findings and the high overall concordance rate, it is possible to conclude that in melanoma in areas with predictable lymphatic drainage, like the extremities and part of the trunk, the particle size of radiotracers for SLN imaging does not play a critical role. However, in complex anatomical regions with multidirectional lymphatic drainage, like head-and-neck area and the upper part of the trunk, SLN imaging using larger colloid particles tends to reduce the detection accuracy. Apparently, here, the increased size impairs the drainage, meaning it is not able to optimally cover all lymph node basins draining from the primary melanoma [14]. The discordance appears to increase with a favor for ICG-$^{99m}$Tc-nanocolloid. The 100% concordance observed in a previous head-to-head evaluation of ICG-$^{99m}$Tc-nanocolloid with $^{99m}$Tc-nanocolloid (25 patients including head-and-neck melanoma) [25] underlines that particle size does influence drainage as observed in the present study. The current data seem to indicate a larger particle size can mean SLNs can be missed in areas of more complex lymphatic drainage, which would result in false negatives of the SLN procedure. This conclusion should, however, be confirmed in a larger series of patients.

Alternative to the use of radiocolloids with a larger particle size, it has been proposed to use radiotracers that have an affinity for CD206 receptors expressed on the surface of macrophages and dendritic cells in lymph nodes and expressed along lymphatic ducts [26]. $^{99m}$Tc-Tilmanocept with a particle size of +7 nm is a dextran particle containing mannosyl units [27]. A trial similar to the one performed in the present study comparing this new generation tracer with the standard radiocolloids for sentinel node work is necessary.

The quest for improvement of SLN targeting with new radiocolloids, simply stated, aims to simplify the role of nuclear medicine imaging in the SLN procedures. While one can argue whether this is desirable or not, there is

**Fig. 4**

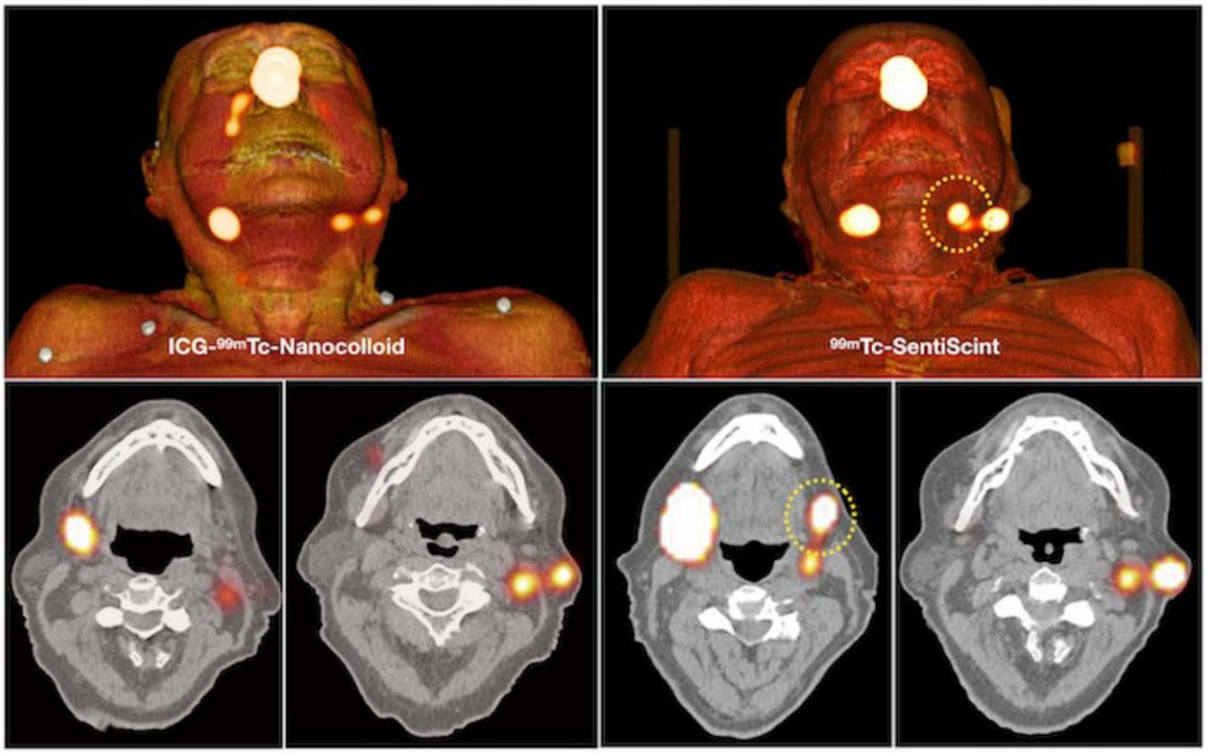


Volume rendered (top) and transaxial (below) SPECT-CT of a patient with a midline nose melanoma showing bilateral neck drainage with tracer concordance for the right side but discordant findings in the left side with a submandibular sentinel lymph node visualized only with $^{99m}$Tc-Senti-Scint (dotted circles). There is some lymph duct visualization lateral from the ICG-$^{99m}$Tc-nanocolloid injection nasal site. ICG, indocyanine green; SPECT-CT, single-photon emission computed tomography combined with computer tomography.

**Fig. 5**

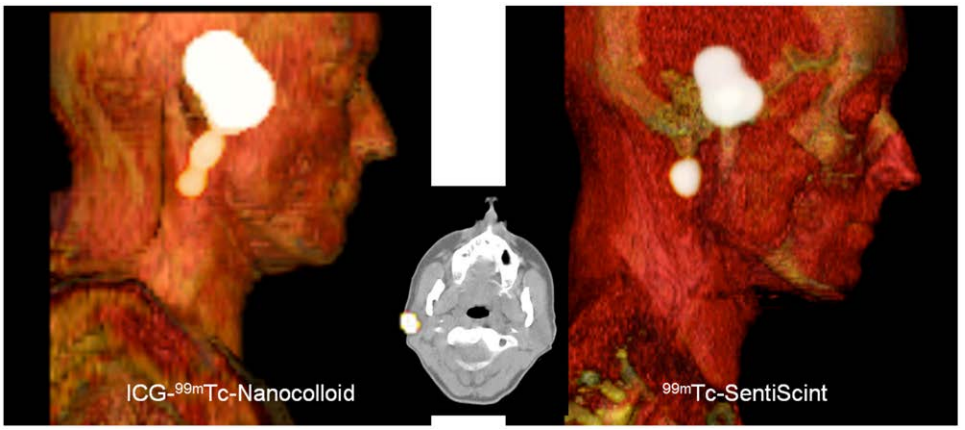


Volume rendered image of a patient with a melanoma of the skin (parietotemporal region). On both images a lymph node is seen region 2 of the neck. The left image (nanocolloid) also shows an SLN between the injection site and the concordant SLN, an SLN in the parotic area. SLN, sentinel lymph node.

a tendency among some surgeons to perform the procedure without the involvement of nuclear medicine. The current data suggest that preoperative mapping using lymphoscintigraphy and SPECT-CT remains today the only imaging modality providing an effective roadmap able to personalize lymphatic imaging. At the up side,

**Fig. 6**

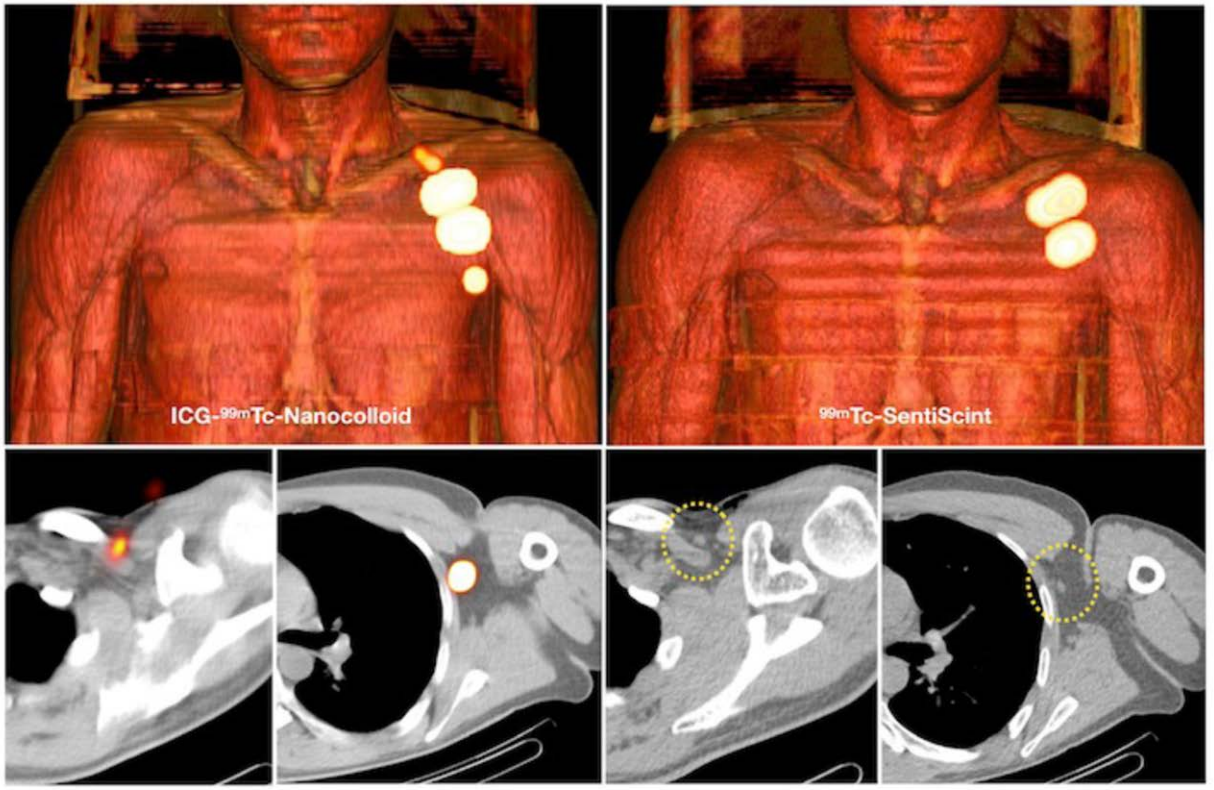


Volume rendered (top) and transaxial (below) SPECT-CT of a patient with a melanoma in the left subclavicular area showing (on the left) drainage to sentinel lymph nodes in the left periclavicular and axillar area on the study performed with ICG-$^{99m}$Tc-nanocolloid. By contrast (on the right), no migration of $^{99m}$Tc-Senti-Scint from the injection site to the above-mentioned nodes (dotted circles) is observed. ICG, indocyanine green; SPECT-CT, single-photon emission computed tomography combined with computer tomography.



the inclusion of fluorescence guidance via ICG-$^{99m}$Tc-nanocolloid makes surgeons prefer use of this tracer (in combination with SPECT-CT) in areas of complex drainage [12]. Hence, it seems that future tracer developments for lymphatic mapping should also aim to address the desire for integrated fluorescence imaging capabilities.

### Conclusion

The hybrid tracer ICG-$^{99m}$Tc-nanocolloid showed a high concordance in lymphatic mapping in comparison to a tracer with significant larger particle size like $^{99m}$Tc-Senti-Scint. Discordant findings were exclusively seen in a minority of patients with complex multidirectional lymphatic drainage, like head and neck, where the hybrid tracer can be of an added value. The slightly higher sentinel node visualization found for ICG-$^{99m}$Tc-nanocolloid was accompanied by depiction of more non-SLNs in some patients. However, the combination of preoperative imaging with the hybrid intraoperative approach adding the fluorescent component to the procedure can help surgeons to effectively identify sentinel nodes at the operation room.

## Acknowledgements

### Conflicts of interest

There are no conflicts of interest.

## References

1 Moncayo VM, Alazraki AL, Alazraki NP, Aarsvold JN. Sentinel lymph node biopsy procedures. *Semin Nucl Med* 2017; **47**:595–617.
2 Faries MB, Thompson JF, Cochran AJ, Andtbacka RH, Mozzillo N, Zager JS, *et al*. Completion dissection or observation for sentinel-node metastasis in melanoma. *N Engl J Med* 2017; **376**:2211–2222.
3 Cabañas RM. An approach for the treatment of penile carcinoma. *Cancer* 1977; **39**:456–466.
4 Morton DL, Wen DR, Wong JH, Economou JS, Cagle LA, Storm FK, *et al*. Technical details of intraoperative lymphatic mapping for early stage melanoma. *Arch Surg* 1992; **127**:392–399.
5 Giammarile F, Alazraki N, Aarsvold JN, Audisio RA, Glass E, Grant SF, *et al*. The EANM and SNMMI practice guideline for lymphoscintigraphy and sentinel node localization in breast cancer. *Eur J Nucl Med Mol Imaging* 2013; **40**:1932–1947.
6 Bluemel C, Herrmann K, Giammarile F, Nieweg OE, Dubreuil J, Testori A, *et al*. EANM practice guidelines for lymphoscintigraphy and sentinel lymph node biopsy in melanoma. *Eur J Nucl Med Mol Imaging* 2015; **42**:1750–1766.
7 Giammarile F, Schilling C, Gnanasegaran G, Bal C, Oyen WJG, Rubello D, *et al*. The EANM practical guidelines for sentinel lymph node localisation in oral cavity squamous cell carcinoma. *Eur J Nucl Med Mol Imaging* 2019; **46**:623–637.

8 Sharma D, Koshy G, Grover S, Sharma B. Sentinel lymph node biopsy: a new approach in the management of head and neck cancers. *Sultan Qaboos Univ Med J* 2017; **17**:e3–e10.

9 Giammarile F, Bozkurt MF, Cibula D, Pahisa J, Oyen WJ, Paredes P, *et al*. The EANM clinical and technical guidelines for lymphoscintigraphy and sentinel node localization in gynaecological cancers. *Eur J Nucl Med Mol Imaging* 2014; **41**:1463–1477.

10 van der Poel HG, Wit EM, Acar C, van den Berg NS, van Leeuwen FWB, Valdes Olmos RA, *et al*.; Sentinel Node Prostate Cancer Consensus Panel Group members. Sentinel node biopsy for prostate cancer: report from a consensus panel meeting. *BJU Int* 2017; **120**:204–211.

11 Mehralivand S, van der Poel H, Winter A, Choyke PL, Pinto PA, Turkbey B. Sentinel lymph node imaging in urologic oncology. *Transl Androl Urol* 2018; **7**:887–902.

12 KleinJan GH, van Werkhoven E, van den Berg NS, Karakullukcu MB, Zijlmans HJMAA, van der Hage JA, *et al*. The best of both worlds: a hybrid approach for optimal pre- and intraoperative identification of sentinel lymph nodes. *Eur J Nucl Med Mol Imaging* 2018; **45**:1915–1925.

13 van den Berg NS, Brouwer OR, Klop WM, Karakullukcu B, Zuur CL, Tan IB, *et al*. Concomitant radio- and fluorescence-guided sentinel lymph node biopsy in squamous cell carcinoma of the oral cavity using ICG-(99m) Tc-nanocolloid. *Eur J Nucl Med Mol Imaging* 2012; **39**:1128–1136.

14 Statius Muller MG, Hennipman FA, van Leeuwen PA, Pijpers R, Vuylsteke RJ, Meijer S. Unpredictability of lymphatic drainage patterns in melanoma patients. *Eur J Nucl Med Mol Imaging* 2002; **29**:255–261.

15 Ballinger JR. The use of protein-based radiocolloids in sentinel node localization. *Clin Transl Imaging* 2015; **3**:179–186.

16 Doepker MP, Yamamoto M, Applebaum MA, Patel NU, Jaime Montilla-Soler M, Sarnaik AA, *et al*. Comparison of single-photon emission computed tomography-computed tomography (SPECT/CT) and conventional planar lymphoscintigraphy for sentinel node localization in patients with cutaneous malignancies. *Ann Surg Oncol* 2017; **24**:355–361.

17 Valdés Olmos RA, Rietbergen DD, Vidal-Sicart S, Manca G, Giammarile F, Mariani G. Contribution of SPECT/CT imaging to radioguided sentinel lymph node biopsy in breast cancer, melanoma, and other solid cancers: from 'open and see' to 'see and open'. *Q J Nucl Med Mol Imaging* 2014; **58**:127–139.

18 McMasters KM, Reintgen DS, Ross MI, Wong SL, Gershenwald JE, Krag DN, *et al*. Sentinel lymph node biopsy for melanoma: how many radioactive nodes should be removed? *Ann Surg Oncol* 2001; **8**: 192–197.

19 Liu LC, Parrett BM, Jenkins T, Lee W, Morita E, Treseler P, *et al*. Selective sentinel lymph node dissection for melanoma: importance of harvesting nodes with lower radioactive counts without the need for blue dye. *Ann Surg Oncol* 2011; **18**:2919–2924.

20 Kroon HM, Lowe L, Wong S, Fullen D, Su L, Cimmino V, *et al*. What is a sentinel node? Re-evaluating the 10% rule for sentinel lymph node biopsy in melanoma. *J Surg Oncol* 2007; **95**:623–628.

21 Vidal-Sicart S, Vera DR, Valdés Olmos RA. Next generation of radiotracers for sentinel lymph node biopsy: what is still necessary to establish new imaging paradigms? *Rev Esp Med Nucl Imagen Mol* 2018; **37**:373–379.

22 Van Den Berg NS, Buckle T, Kleinjan GI, Klop WM, Horenblas S, Van Der Poel HG, *et al*. Hybrid tracers for sentinel node biopsy. *Q J Nucl Med Mol Imaging* 2014; **58**:193–206.

23 Boxen I, McCready D, Ballinger JR. Sentinel node detection and definition may depend on the imaging agent and timing. *Clin Nucl Med* 1999; **24**:390–394.

24 De Cicco C, Cremonesi M, Luini A, Bartolomei M, Grana C, Prisco G, *et al*. Lymphoscintigraphy and radioguided biopsy of the sentinel axillary node in breast cancer. *J Nucl Med* 1998; **39**:2080–2084.

25 Brouwer OR, Buckle T, Vermeeren L, Klop WM, Balm AJ, van der Poel HG, *et al*. Comparing the hybrid fluorescent-radioactive tracer indocyanine green-99mTc-nanocolloid with 99mTc-nanocolloid for sentinel node identification: a validation study using lymphoscintigraphy and SPECT/CT. *J Nucl Med* 2012; **53**:1034–1040.

26 Engering AJ, Cella M, Fluitsma D, Brockhaus M, Hoefsmit EC, Lanzavecchia A, Pieters J. The mannose receptor functions as a high capacity and broad specificity antigen receptor in human dendritic cells. *Eur J Immunol* 1997; **27**:2417–2425.

27 Sondak VK, King DW, Zager JS, Schneebaum S, Kim J, Leong SP, *et al*. Combined analysis of phase III trials evaluating [$^{99}$mTc]tilmanocept and vital blue dye for identification of sentinel lymph nodes in clinically node-negative cutaneous melanoma. *Ann Surg Oncol* 2013; **20**:680–688.